

Supporting Information

Dendritic Hollow Nitrogen–Doped Carbon Nano Spheres for Oxygen Reduction at Primary Zinc-Air Battery

J. Anjana, Anook Nazer Elelath and Azhagumuthu Muthukrishnan*

School of Chemistry, Indian Institute of Science Education and Research Thiruvananthapuram,
Maruthamala (P.O.), Vithura, Thiruvananthapuram 695 551, Kerala, India.

Email: muthukrishnan@iisertvm.ac.in

TABLE OF CONTENTS

S. No.	Contents	Page No.
Figure S1	Powder X-ray diffraction spectroscopy.....	S2
Figure S2	Raman spectroscopy.....	S3
Figure S3	X-ray photoelectron survey spectra.....	S4
Figure S4	Deconvoluted C-1s XPS spectra.....	S5
Figure S5	TEM images of the silica templates.....	S6
Figure S6	SEM and TEM images of the N-doped carbon materials.....	S7
Figure S7	TGA curves of the N-doped carbon materials.....	S9
Figure S8	BET isotherm and particle size distribution plots.....	S10
Figure S9	RRDE voltammograms of ORR on N-doped carbon materials at different rotational speeds.....	S11
Figure S10	Discharge polarization curves and specific capacity curve of Benchmark Pt/C catalysts.....	S12
Table S1	Table of atomic weight percentage of nitrogen from N-1s XPS spectra.....	S13
Table S2	Table of BET surface area and other details	S14

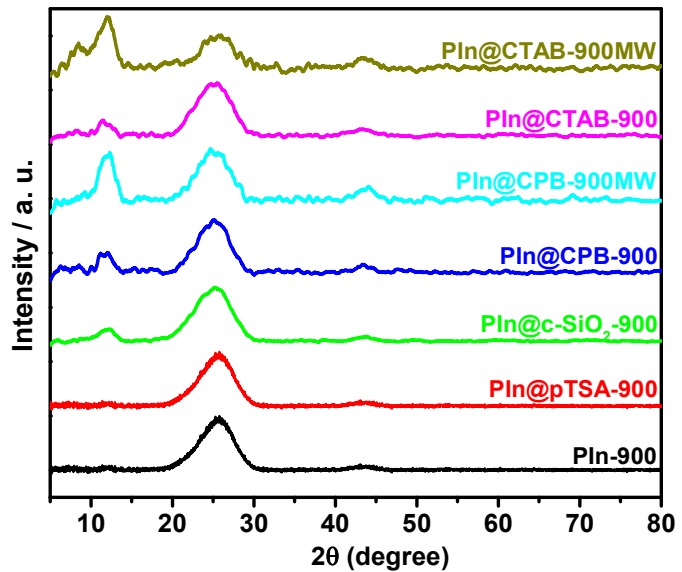


Figure S1. The powder X-ray diffraction patterns of synthesized compounds

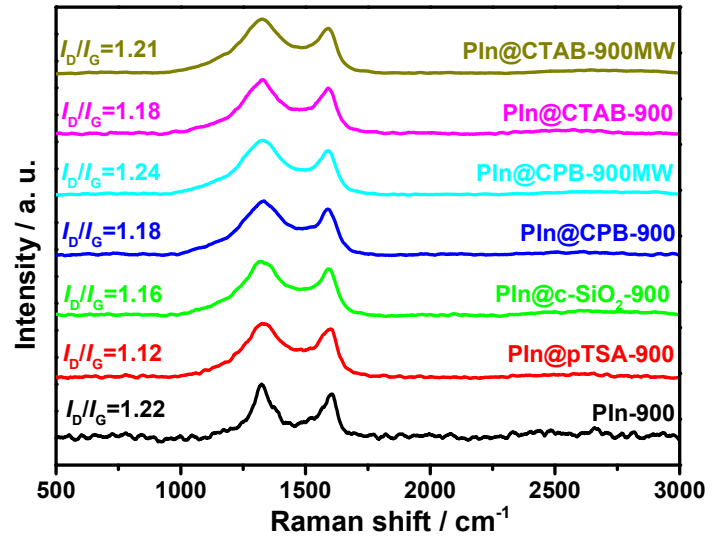


Figure S2. Raman spectra of the synthesized N-doped carbon compounds

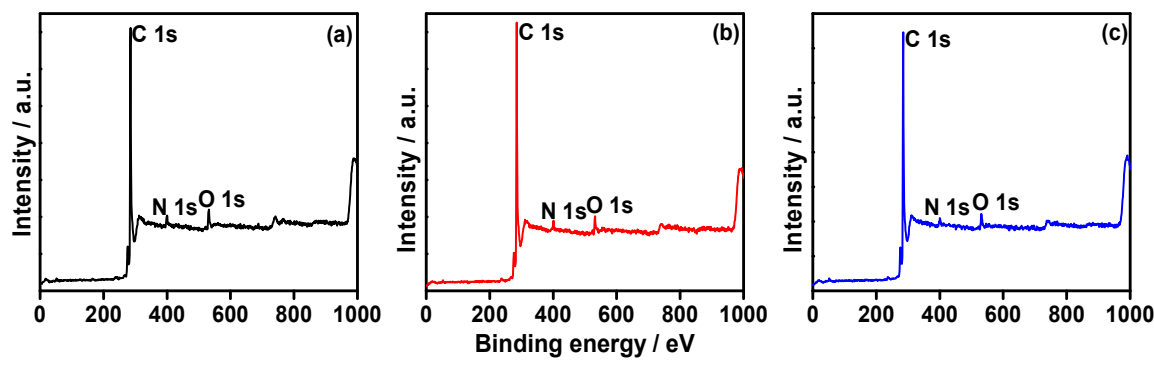


Figure S3. The XPS survey spectra of (a) PIn@c-SiO₂-900, (b) PIn@CTAB-900 and (c) PIn@CPB-900

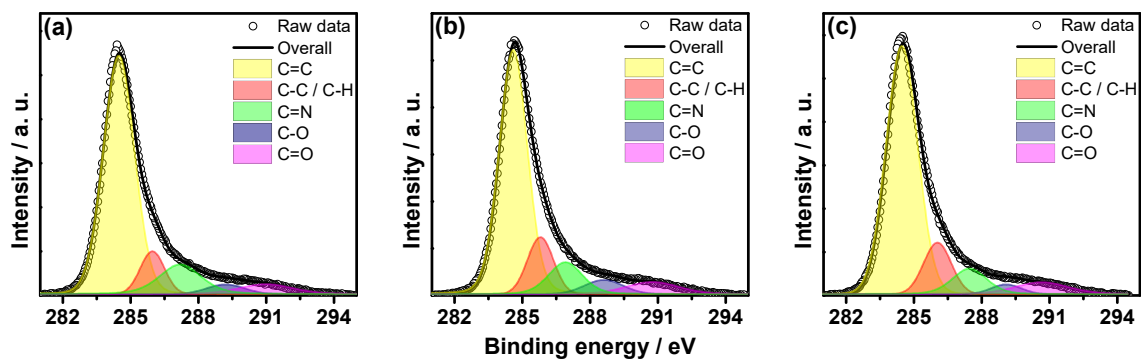


Figure S4. The core-level C 1s XPS spectra of (a) PIn@c-SiO₂-900, (b) PIn@CTAB-900 and (c) PIn@CPB-900

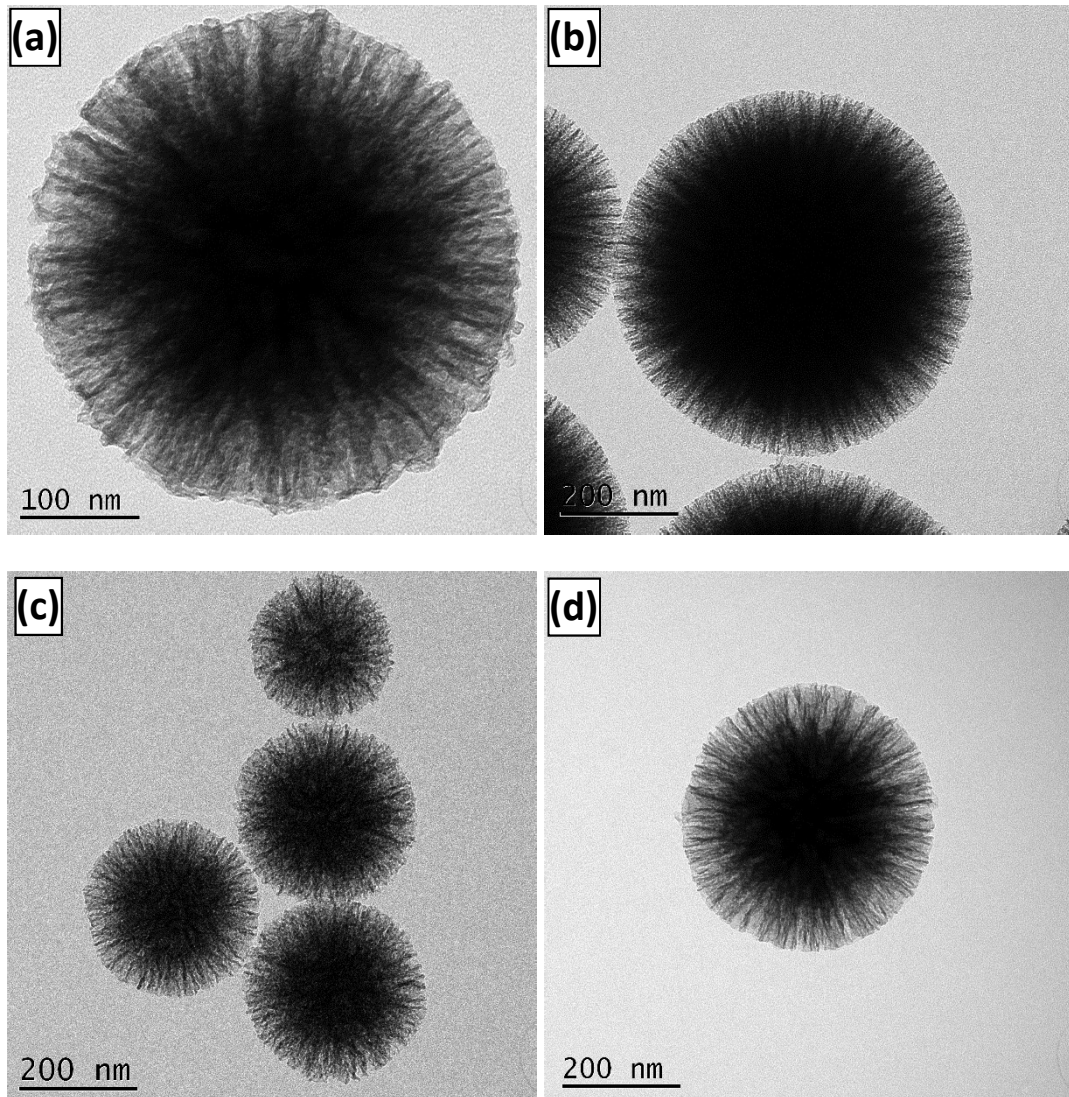
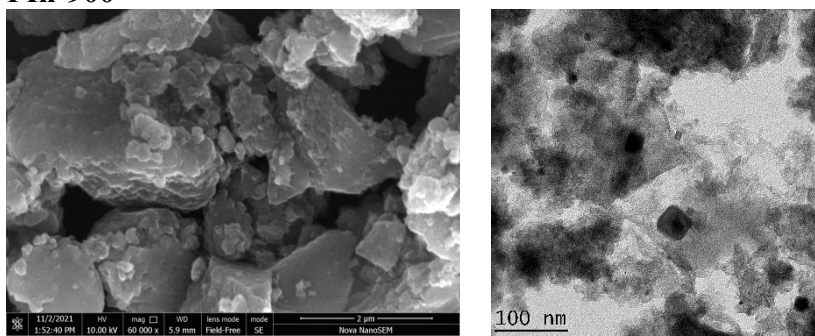
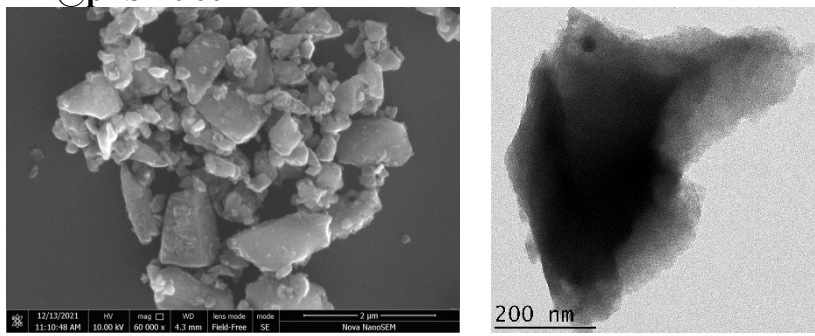


Figure S5. TEM images of the Dendritic porous nano-silica templates using CPB templates (a) autoclave and (b) microwave methods; CTAB template (c) autoclave and (d) microwave methods.

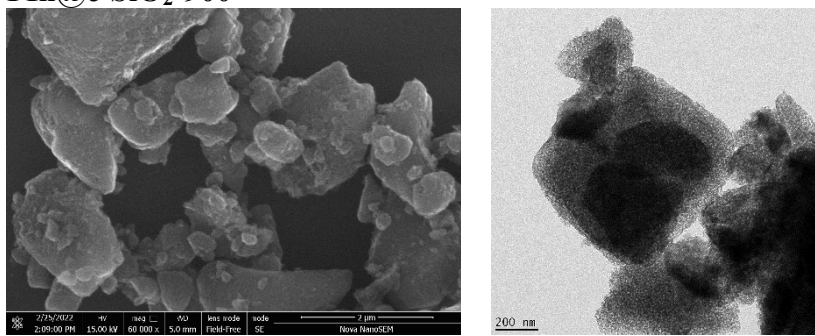
PIn-900



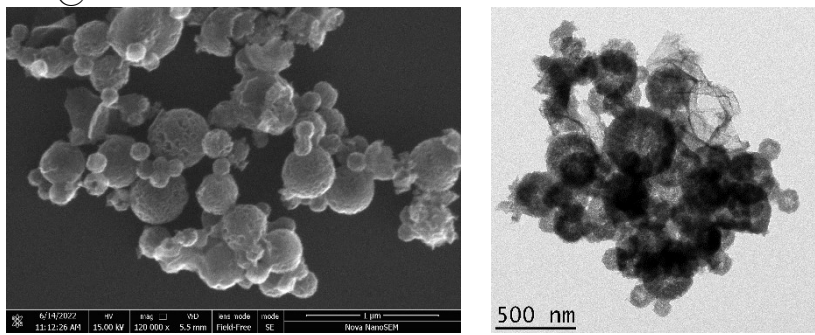
PIn@pTSA-900



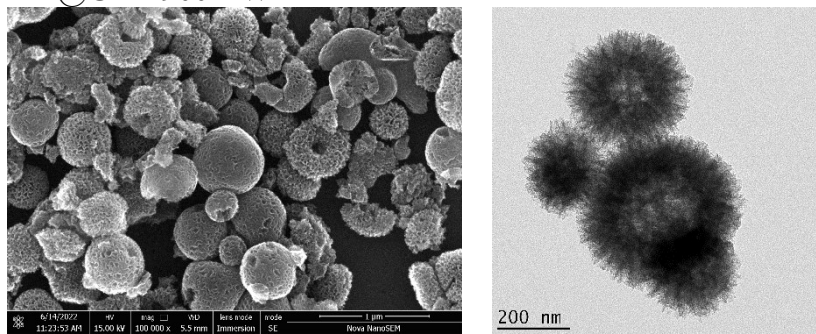
PIn@c-SiO₂-900



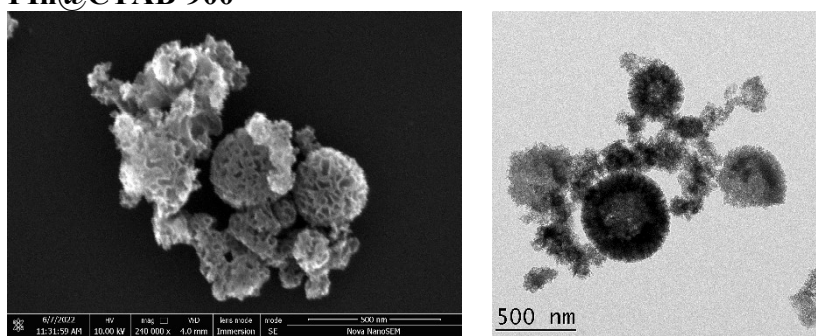
PIn@CPB-900



PIn@CPB-900MW



PIn@CTAB-900



PIn@CTAB-900MW

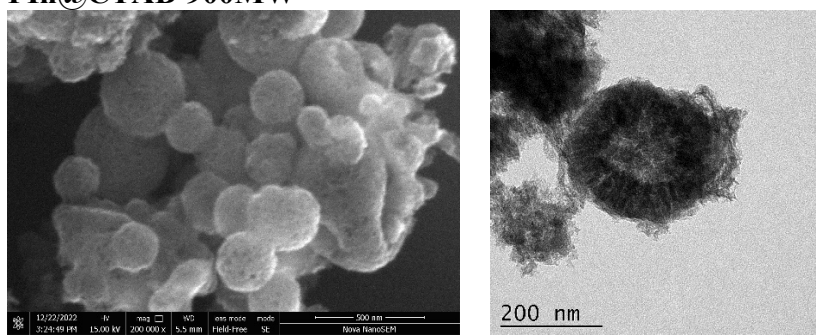


Figure S6. The SEM and TEM images of synthesized N-doped carbon materials

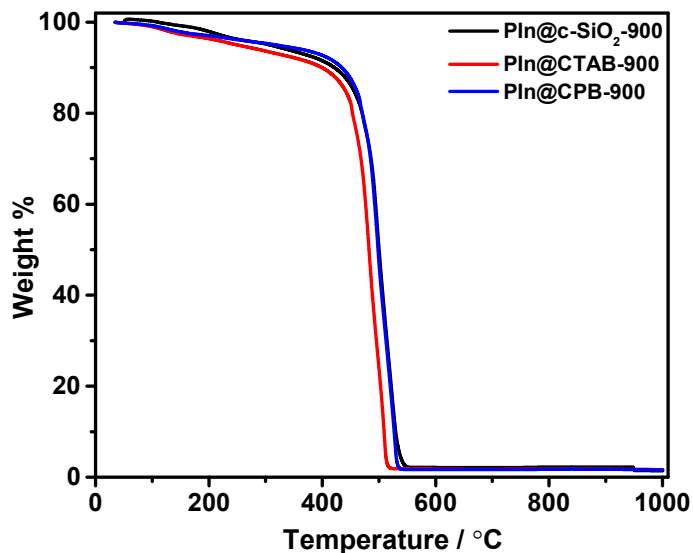


Figure S7. The Thermogravimetric analysis (TGA) curves of catalyst materials showing a trace amount of Fe species

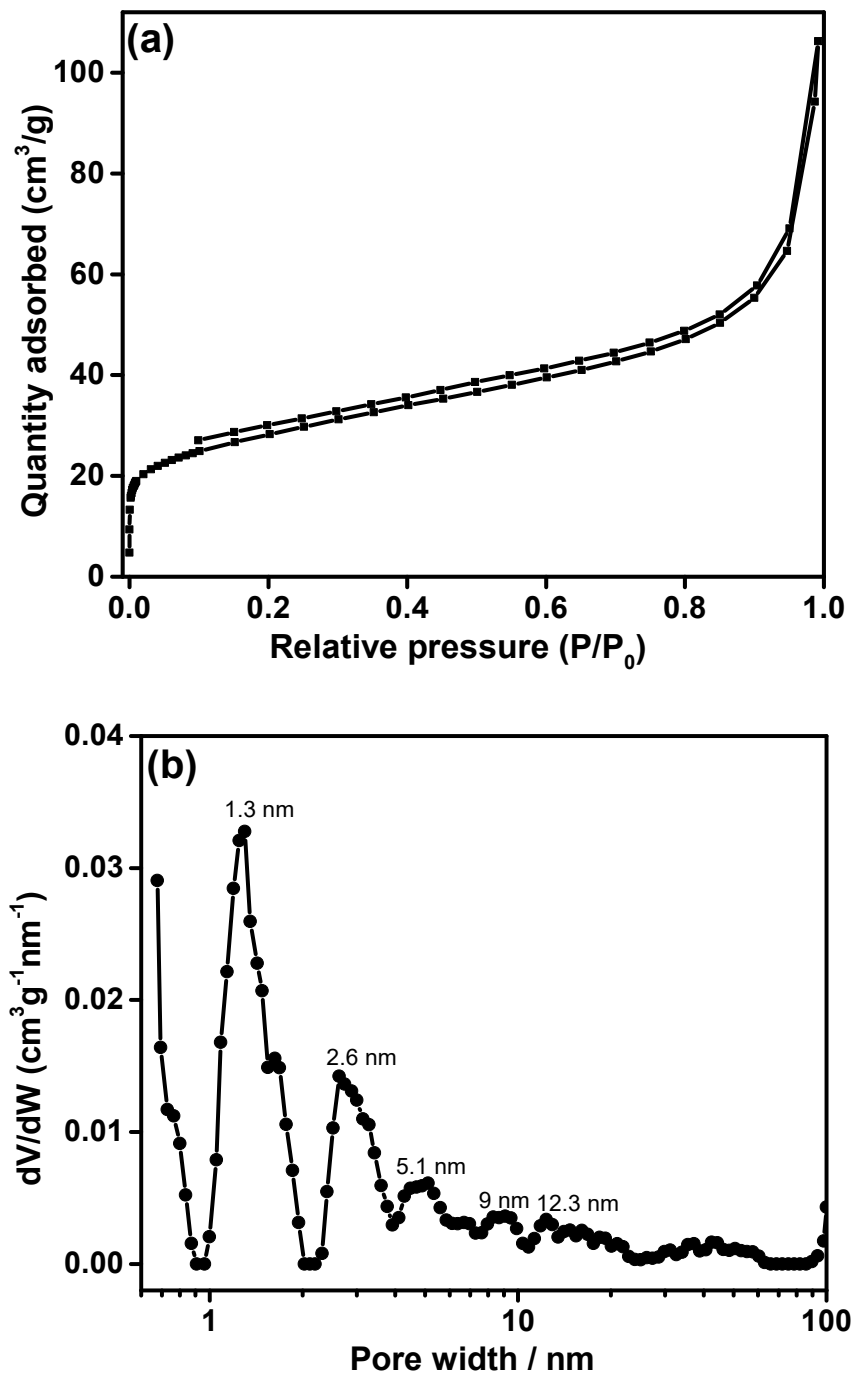


Figure S8. The N_2 -adsorption isotherm and the particle size analysis using NLDFT analysis of PIn-900.

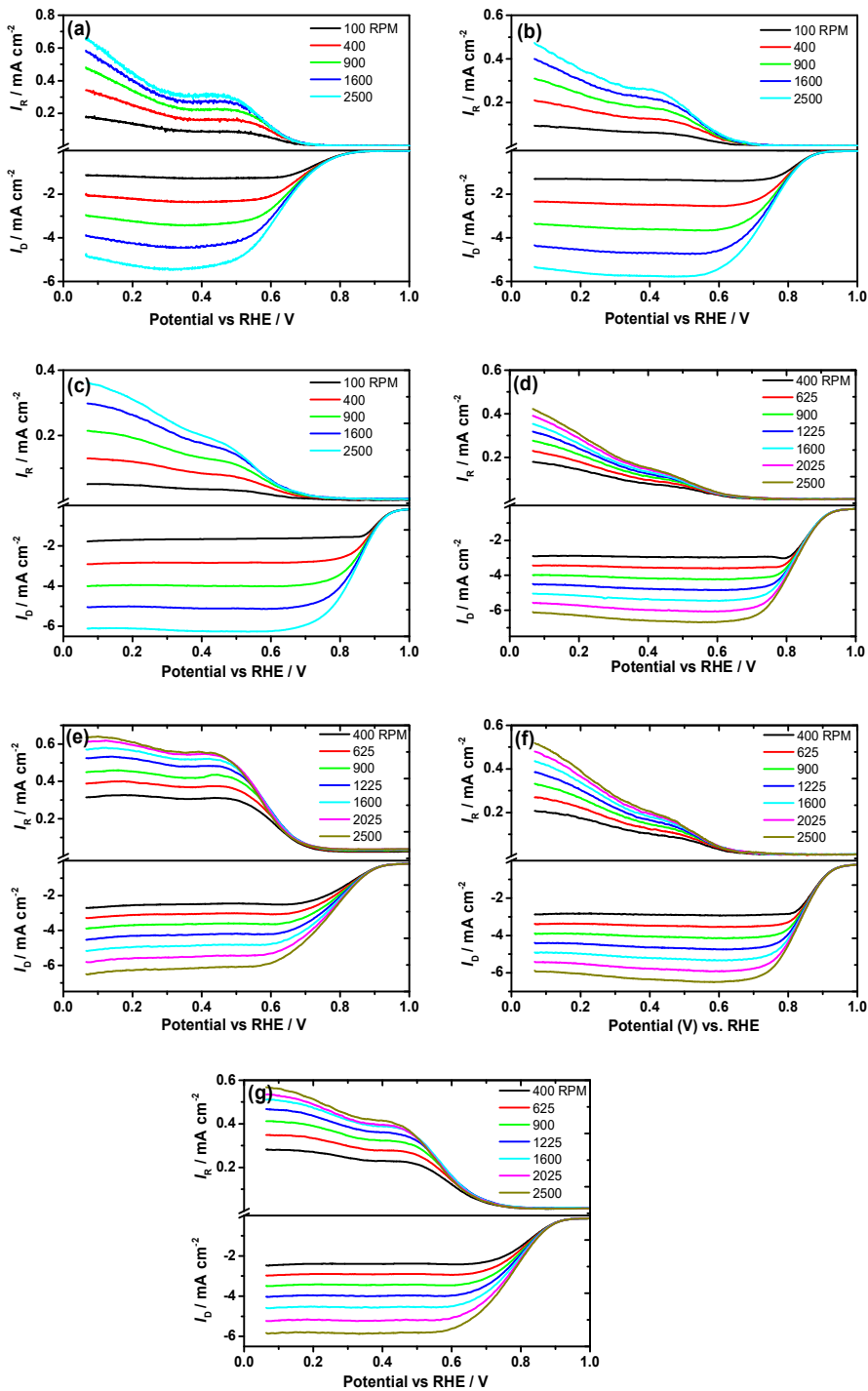


Figure S9. RRDE voltammograms of ORR on different carbon materials at O_2 -saturated 0.1 M KOH electrolyte. The scan rate is 10 mVs^{-1} . (a) PIn-900, (b) PIn@p-TSA-900, (c) PIn@c-SiO₂-900, (d) PIn@CPB-900, (e) PIn@CPB-900MW, (f) PIn@CTAB-900 and (g) PIn@CTAB-900MW

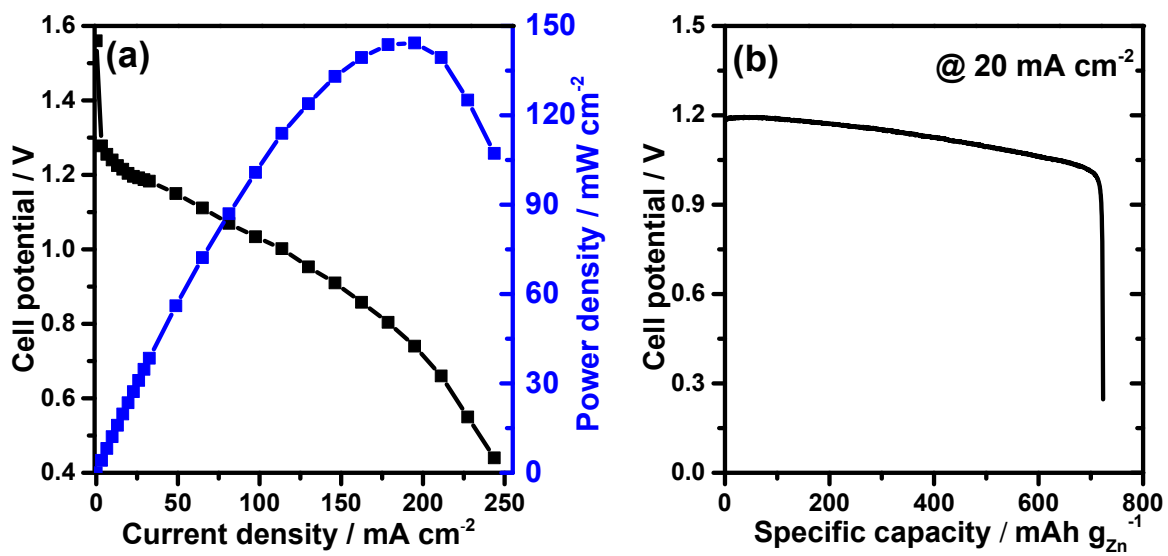


Figure S10. (a) Discharge polarisation curve of the benchmark Pt/C catalysts (loading density: $50 \mu\text{g}_{\text{Pt}}\text{cm}^{-2}$). The right y-axis and the blue line refer to the power density values. (b) Discharge chronopotentiometry curves at a constant current of 20 mA cm^{-2} .

Table S1. Percentage of different types of nitrogen obtained from XPS data

Compound	Py-N (%)	Gr-N (%)	Pr-N (%)	N-O (%)
PIn@c-SiO ₂ -900	20.66	50.36	15.51	13.47
PIn@CTAB-900	19.17	53.25	11.47	16.12
PIn@CPB-900	19.44	55.48	12.03	13.04

Py-N – Pyridinic, Pr – pyrrolic, Gr – graphitic, N-O – nitrogen oxides

Table S2. Estimated total and micropore (t-plot) and mesopore (BJH) surface area and the micropore volume from BET adsorption isotherm analysis

Compounds	Onset potential (V)	Surface area (m^2g^{-1})	t-plot micropore area (m^2g^{-1})	t-plot micropore volume (cm^3g^{-1})	BJH desorption pore area (m^2g^{-1})
PIn-900	0.87	93.5	19.4	0.011	24.5
PIn@pTSA-900	0.93	590.6	371.7	0.251	135.2
PIn@c-SiO ₂ -900	1.00	786.8	367.7	0.156	540.0
PIn@CTAB-900	0.99	850.7	398.3	0.172	192.3
PIn@CTAB-900MW	0.94	1330.8	191.0	0.052	658.4
PIn@CPB-900	0.97	955.2	184.4	0.098	409.3
PIn@CPB-900MW	0.94	1286.6	133.0	0.033	601.5